



HAL
open science

Size effects in cobalt plastically strained in tension: impact on gliding and twinning work hardening mechanisms

Eric Hug, Clément Keller, Pierre-Antoine Dubos, Mayerling Martinez Celis

► To cite this version:

Eric Hug, Clément Keller, Pierre-Antoine Dubos, Mayerling Martinez Celis. Size effects in cobalt plastically strained in tension: impact on gliding and twinning work hardening mechanisms. Journal of Materials Research and Technology, 2021, 11, pp.1362-1377. 10.1016/j.jmrt.2021.01.105 . hal-03137062

HAL Id: hal-03137062

<https://hal.science/hal-03137062>

Submitted on 13 Feb 2023

HAL is a multi-disciplinary open access archive for the deposit and dissemination of scientific research documents, whether they are published or not. The documents may come from teaching and research institutions in France or abroad, or from public or private research centers.

L'archive ouverte pluridisciplinaire **HAL**, est destinée au dépôt et à la diffusion de documents scientifiques de niveau recherche, publiés ou non, émanant des établissements d'enseignement et de recherche français ou étrangers, des laboratoires publics ou privés.



Distributed under a Creative Commons Attribution - NonCommercial 4.0 International License

Size effects in cobalt plastically strained in tension: impact on gliding and twinning work hardening mechanisms

Eric Hug^{a*}, Clément Keller^b, Pierre-Antoine Dubos^c, Mayerling Martinez Celis^a

^aLaboratoire de Cristallographie et Sciences des Matériaux, ENSICAEN, Université de Caen, CNRS, 6 Bd
Maréchal Juin, 14050 Caen France

^bGroupe de Physique des Matériaux, UMR 6634 CNRS - Université de Rouen, INSA de Rouen, avenue de
l'université, 76800 Saint-Etienne du Rouvray, France

^cUniversité de Nantes, Institut de Recherche en Génie Civil et Mécanique (UMR CNRS 6183), 58 rue Michel
Ange – BP 420, 44606 Saint-Nazaire Cedex, France

Corresponding author:

*Eric HUG, Professor
Tel: +33 2 31 45 13 13
Fax: +33 2 31 95 16 00
e-mail: eric.hug@ensicaen.fr

Abstract

Mechanical properties in tension of cobalt have been studied in a wide range of grain size d using thickness t of samples from 125 to 700 μm . The Hall and Petch (HP) relationship indicates that the yield stress strongly varies for t/d below a critical value around 14, highlighting the existence of a multicrystalline regime. The behavior becomes almost single crystalline when t/d is lower than 2.5, with a very small HP slope. The reduction of the t/d ratio has also a large influence on the work hardening of cobalt, especially in the beginning of plasticity, which mainly corresponds to the stage of basal slip mechanisms. However,

these size effects tend to vanish when twinning becomes predominant. Nanoindentation measurements and application of a simple composite model show that the appearance of the multicrystalline regime is closely related to surface effects that develop through the thickness of the specimens. In addition, the **Kocks - Mecking** work hardening model predicts a significant increase of the average free path of dislocations in the basal slip stage. A quantitative analysis of dislocation pile-ups that develop during this stage supports the hypothesis that the mechanical softening observed in cobalt multicrystals is related to a higher activity of dislocations, which can escape more easily on free surfaces. When twinning becomes the main deformation mechanism, dislocation glide is restricted which reduced, in turn, the surface effect. Consequently, size effects gradually disappear with hardening.

Keywords

cobalt; size effects; mechanical properties; dislocations; basal slip mechanisms; twinning

1. Introduction

Forming process of thin metallic parts of miniaturized systems used in medical or electrical devices remains an issue for obtaining desired performances in terms of structural and functional properties. The influence of free surfaces on the properties of the material becomes very sensitive when one or several characteristic length of the representative volume element becomes less than typically a few hundred of micrometers [1]. Such intrinsic size effect is moreover strongly dependent on the grain size [2, 3] and leads to an impact of thickness (t) to grain size (d) ratio t/d on the mechanical properties [4, 5]. The

flow stress, the work hardening mechanisms and the fracture properties are modified when t/d decreases below a critical value. This t/d threshold is linked to the stacking fault energy [6], and some experimental conditions such as the temperature [7], the strain level [8], and the mechanical loading [9, 10]. The surface effect is quite well understood for face centered cubic (fcc) metals and alloys and is intimately related to a stress gradient of typically 30% between core and surface grains [11]. This was highlighted by **transmission electron microscopy** (TEM) and nanohardness experiments and confirmed by finite element simulations using strain gradient crystal plasticity models [12]. Further decrease on the t/d ratio leads to the existence of a second critical ratio, around unity [5, 13], related to a constant stress regime dependent of the thickness [14, 15].

The progressive transition from a polycrystalline to a quasi-single crystalline state, through an intermediate so-called multicrystalline state, strongly modifies the mechanical properties and affects **not only** the forming performances of small metallic parts [16, 17], but also their functional **properties, such** as the coercive field strength and magnetic behavior [18, 19], the electrical resistivity [20, 21] or the thermal **conductivity** [22]. Such mechanisms associated with the strengthening of fcc materials are well documented in the literature but their characterization for others crystallographic structures remains, however, an issue. Many researches focused on the so-called “smaller is stronger” effect depicted by micropillar experiments on **hexagonal closed packed** (hcp) metals [23, 24]. However, very few works concerning size effects in hcp crystallographic structures are available in the range of laminated part thickness. The grain size impact on the yield stress verifies a Hall and Petch (HP) relationship, as shown for instance for magnesium [25], zirconium [26] and titanium [27]. Concerning magnesium, this law was found to be valid for higher values of

plastic strains by Ono *et al* [28], but only five grain diameter values were used to plot the HP graphs. Grain size was also found to influence twinning [29] and fracture mechanisms [30] of hcp metals. Twinning and gliding regimes exhibit their own HP relationship with higher slopes in twinning mechanisms as dislocation gliding is restricted in this case. HP plots with two or three distinct regimes were depicted [31] depending on the plastic strain level and the dominant work hardening mechanism. For a given grain size, Lou *et al* [32] have shown that a decrease in thickness of Mg alloys leads to a decrease in the ultimate stress in tension and a corresponding decrease in the fracture strain. Same evolutions were obtained for titanium plastically strained in tension but also in shear [33]. To the knowledge of the authors, only one major work was dedicated to the coupled effect of the grain size and t/d ratio for hcp materials. This study was devoted to zinc [34], and a critical t/d ratio of 12 was found below that one a softening of the mechanical properties was observed. This effect was attributed to the impact of a strong basal texture which develops during plastic deformation.

Among all hcp structures, cobalt has been much less studied but is of particular interest due to its specific mechanical and magnetic **properties**, which makes it a good candidate for miniaturized systems and components. Cobalt deserves also attention due to its higher melting point and very low stacking fault energy compared with others hcp metals [35]. Work hardening curves of polycrystalline cobalt exhibit two distinct stages in the plasticity regime. Basal dislocation glide on the crystallographic system $\{0001\}\langle 1\bar{2}10 \rangle$ is the dominant mechanism in the first stage of work hardening (labelled stage A in the following). Unlike magnesium, where prismatic or pyramidal slip systems can also be observed under specific experimental conditions [36, 37], basal slip is the only activated

mode in cobalt [38, 39]. After an amount of plastic strain, because of the limited number of available slip systems, twinning process occurs in the second work hardening stage (stage B) as an alternative for plastic deformation. Several twinning modes occur in cobalt but twinning in the $\{10\bar{1}2\}$ planes was found to be the majority mode [40] due to its low corresponding twinning shear [41]. The size effects in such metal, for instance the impact of the t/d ratio on gliding and twinning regimes, deserve attention.

The objective of this work is to contribute to the understanding of size effects in metallic materials by giving first new experimental results concerning high purity cobalt. **HP** formalism and strengthening mechanisms were studied and size effects were depicted in the gliding regime below a critical t/d ratio related to the low stacking fault energy in a similar way than for fcc alloys. This behavior fades away when twinning occurs. Surface effects were highlighted by nanoindentation experiments completed by the application of a simple composite model [42]. The softening of the mechanical properties observed in the stage A of work hardening is finally discussed using the Kocks-Mecking formalism [43, 44] and the observation of dislocation pile-ups against boundaries in the gliding planes.

2. Experimental details

Laminated sheets of high purity cobalt (higher than 99.9wt.%) of variable thicknesses t ranging from 125 to 700 μm , provided by GoodFellow company, were considered. As-received sheets were first annealed at 900 °C for 1 h and considered as the starting polycrystalline state. Samples were therefore **subjected** to heat treatments at 1100 °C with increasing times in order to modify the grain size d and the corresponding t/d

ratio. For all heat treatments, the partial pressure of oxygen was maintained lower than 10^{-7} mbar for limiting oxidation of the free surfaces during the annealing process. Cobalt exhibits an allotropic transformation at 376 °C during cooling, between the hcp phase and the fcc high temperature metastable structure. A slow cooling of samples inside the furnace during 24 h is mandatory in order to control the amount of remaining secondary fcc phase. Values of d for different thicknesses and corresponding t/d ratios are given in Table I.

Table I. Extreme values d_{min} and d_{max} of mean grain sizes obtained by annealing of cobalt with various thicknesses t (standard deviation is about one-half of the grain size) associated with their corresponding t/d ratio ranges.

t (μm)	d_{min} (μm)	d_{max} (μm)	t/d range
125	30	57	2.2 – 4.2
250	72	248	1 – 3.5
500	10	119	4.5 - 44
700	10	112	6 - 70

Uniaxial monotonous tensile experiments were carried out up to fracture, using an Instron 5569 (Norwood, MA, USA) universal testing machine, on dog bone shaped samples with a gauge length of 20 mm. Strain measurements were achieved by a clip-on extensometer for all thicknesses except for the 125 μm thickness, for which a laser extensometer was used to avoid buckling and surface fracture initiator. The strain rate was maintained in the range $(10^{-4} - 10^{-3}) \text{ s}^{-1}$ using a constant crossing head speed of 1 mm/min. All tests were performed with the tensile axis aligned with the rolling direction. Between

three and six mechanical tests were carried out for each metallurgical state and average stress values were reported on HP plots and work hardening curves. As mentioned in previous works of our group [18, 45], a χ^2 statistical test was systematically performed on the least square regression considering one or two different stages for HP plots. An error bar of 5% was associated with each stress measurement in agreement with the experimental scattering analysis. Supplementary interrupted tensile tests were performed at different stages of strengthening, to analyze the deformation mechanisms using optical and electron microscopy. Nanoindentation measurements through the thickness of some samples, using a staggered matrix, were performed with a MTS XP nanoindentation device to capture the softening effect of free surfaces in polycrystalline specimens. Berkovich diamond tip (nominal tip radius of curvature of 20 nm) was employed and measurements were displacement-controlled up to a penetration depth of 500 nm. Spacing between each indent was set to 1 μm to avoid interaction between plastic zones. A calibration experiment on a fused quartz specimen was performed before each test to ensure reliable measurements.

Grain size, crystallographic texture and residual fcc phase fraction were systematically evaluated by electron back scattered diffraction (EBSD) working on a scanning electron microscope (SEM). Gliding mechanisms, dislocation features and pile-ups were studied by TEM with a microscope operating at 200 kV. To this aim, 3 mm diameter discs were first extracted from mid-thickness of the strained specimens and then thinned down by mechanical polishing and electropolishing using a twin jet electrolytic thinning apparatus (90% glacial acetic acid and 10% perchloric acid solution, working voltage of 50 V).

3. Experimental results

3.1. Microstructural evolution of cobalt samples with heat treatments

Fig. 1 presents a general overview of the microstructure of polycrystalline and multicrystalline samples after heat treatment. Independently of the t/d ratio, a well-defined hcp crystallographic structure is evidenced giving an isotropic grain size both through the thickness (Fig. 1(a)) and on the surface (Fig. 1(b)). Specimens also exhibit $71.4^\circ/\langle 1\bar{2}10 \rangle$ boundaries resulting from the martensitic transformation from fcc to hcp during cooling.

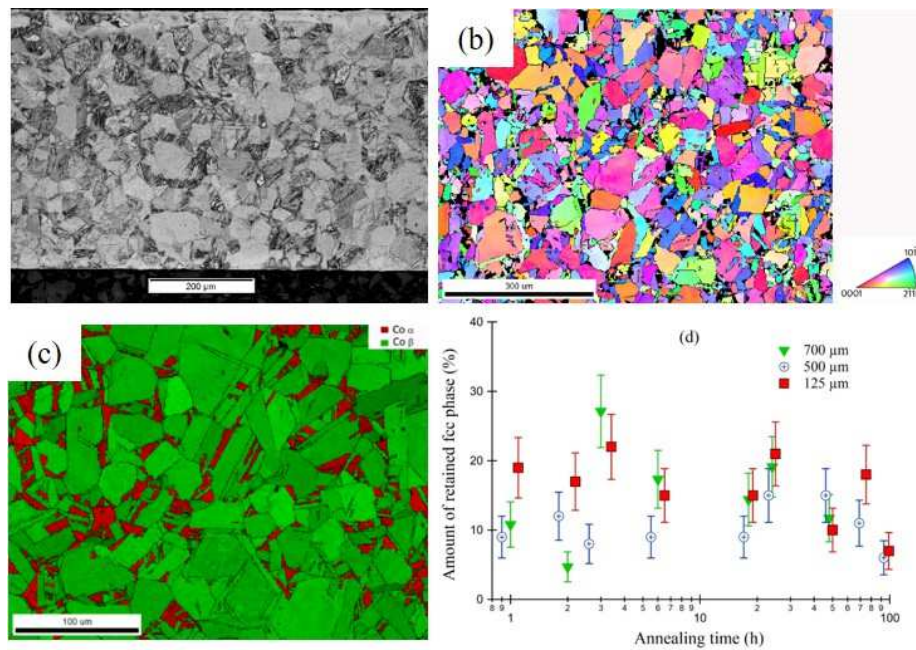


Figure 1 – General overview of the microstructure of cobalt, unstrained state. (a) Grain size across the thickness, SEM, $t/d = 14$. (b) EBSD IPF map of the hcp phase, $t/d = 14$. (c) Cartography representing in red the hcp phase and in green the fcc one ($t/d = 19$). (d) Amount of residual fcc phase with the holding time of annealing at $T = 1100^\circ\text{C}$, for three thicknesses of cobalt samples.

The retained fcc phase is mainly located at triple junctions of grain boundaries of the hcp phase as revealed by EBSD cartography (Fig. 1(c)). This secondary phase modifies the mechanical properties of cobalt for amounts of the order of 40-45 % [46] well higher than the values displayed in Fig. 1(d) (between 5 % and 25 %, depending on the t/d ratio). We will consider in the following paragraphs that modifications of the mechanical properties of cobalt result to the behavior of the hcp phase only.

Fig. 2 represents the c-axis pole figures for cobalt specimens with various t/d ratio. It can be shown that the crystallographic texture of the hcp phase does not significantly vary with heat treatments or t/d ratio. The basal $\{0001\}$ texture, with basal poles $\pm 30-60^\circ$ away from the normal direction (ND), is always present. Maximal texture density expressed in multiples of a random distribution takes values between 4 and 9.

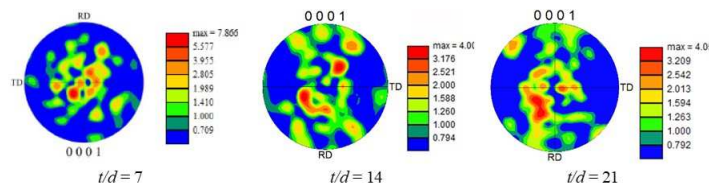


Figure 2 – Pole figures for annealed cobalt samples with various t/d ratio.

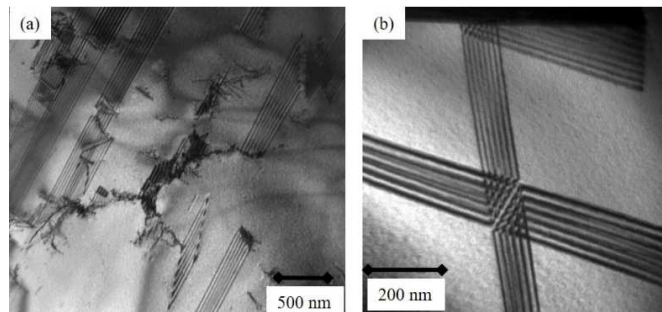


Figure 3 – Stacking faults observed in (a) hcp and (b) fcc phases of unstrained cobalt.

The initial microstructure is also characterized by the existence of numerous stacking faults, both in hcp and fcc phases (Fig. 3). These faults are bounded by partial dislocations and their occurrence reveals the low stacking fault energy of cobalt, typically in the range 23-31 mJ/m² [47].

3.2. Mechanical behavior of cobalt in tension. Impact of the t/d ratio

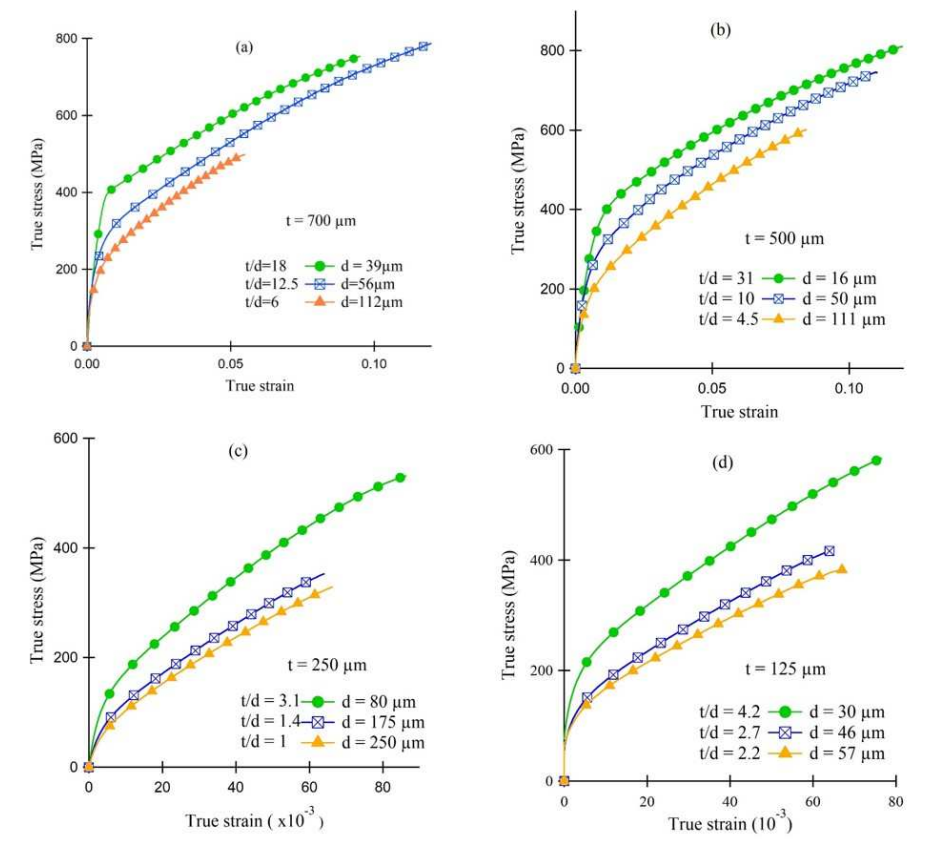


Figure 4 – Typical true stress - true strain curves obtained in cobalt with various t/d ratio and a thickness of (a) 700 μm , (b) 500 μm , (c) 250 μm and (d) 125 μm .

Figure 4 displays some examples of tensile curves of cobalt, obtained for the four thicknesses and variable grain size and t/d ratio. All samples in the starting state (black circle curves) exhibit a yield stress typically between 200 and 400 MPa, followed by a relatively large work hardening. The maximum stress level can reach values of 800 MPa, for ultimate deformation (before necking) in the range 0.06 – 0.1.

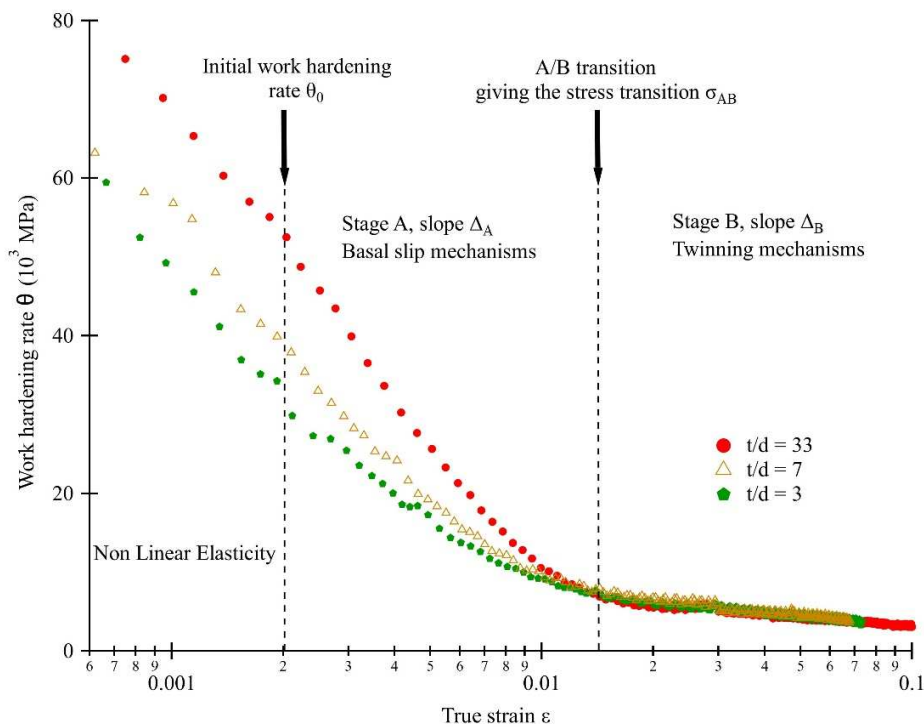


Figure 5 – Examples of hardening curves for polycrystalline ($t/d = 22$), multicrystalline ($t/d = 7$) and quasi single crystalline ($t/d = 3$) cobalt with corresponding work hardening stages.

In order to go further into the plasticity mechanisms, it is of major importance to consider the mechanisms linked to gliding and those due to twinning. In general for hcp

metals, strain mechanisms in small grain specimens are driven by slip processes whereas for larger ones deformation twinning becomes predominant [48]. These two deformation mechanisms can be evidenced and studied by considering work-hardening plots issued from monotonous tensile curves. Figure 5 displays typical work hardening curves $\theta(\varepsilon) = d\sigma/d\varepsilon$ for polycrystalline, multicrystalline and quasi single crystalline specimens with θ the work hardening rate. All curves exhibit a nonlinear elasticity regime (not studied in this work) followed by two distinct hardening stages A and B, separated by a threshold stress σ_{AB} . These stages are traditionally encountered in hcp structures and are linked to gliding mechanisms and twinning processes, respectively.

It can be considered, in first approach, a linear relationship between θ and ε in stages A and B, represented by corresponding slopes Δ_A and Δ_B . Both slopes are negative highlighting the general decrease in work hardening rate with plastic deformation. However, this effect is much pronounced when slip mechanisms predominate. As shown in Fig. 5, Δ_A also strongly decreases (in absolute value) with t/d ratio, together with the work hardening rate θ_0 at the beginning of the plasticity (*i.e.* for a plastic strain of 0.002). In the twinning stage, Δ_B remains more or less independent of t/d ratio.

3.3. Effect of the t/d ratio on the HP relationship

Based on the monotonous tensile curves exhibited in Fig. 4, HP plots are illustrated Fig. 6, for various plastic deformations and three thicknesses. Two distinct linear regimes are evidenced for the 0.5 mm thick specimens (Fig. 6(a)), from the very beginning of the plasticity. The two regimes correspond to the polycrystalline and the multicrystalline

behaviors. A linear regression on the two regimes allows us to compute the HP coefficients k and σ_0 of the HP relationship, which links the flow stress σ to the strain level ε and the grain size d [49]:

$$\sigma(\varepsilon) = \sigma_0(\varepsilon) + \frac{k(\varepsilon)}{\sqrt{d}} \quad (1)$$

$\sigma_0(\varepsilon)$ and $k(\varepsilon)$ are material parameters and function of the strain. For the yield stress ($\varepsilon_p = 0.002$), when t/d ratio is higher than a critical value $(t/d)_c = 14$, HP constants for cobalt in the polycrystalline regime take values $k_p = 245 \text{ MPa}\cdot\mu\text{m}^{1/2}$ and $\sigma_{0p} = 211 \text{ MPa}$, in accordance with the few experimental results available in open literature [50]. When $t/d < 14$, k takes higher values ($k_m = 1590 \text{ MPa}\cdot\mu\text{m}^{1/2}$) than for polycrystalline specimens, indicating a much more pronounced grain size dependence of the stress in this so-called multicrystalline regime.

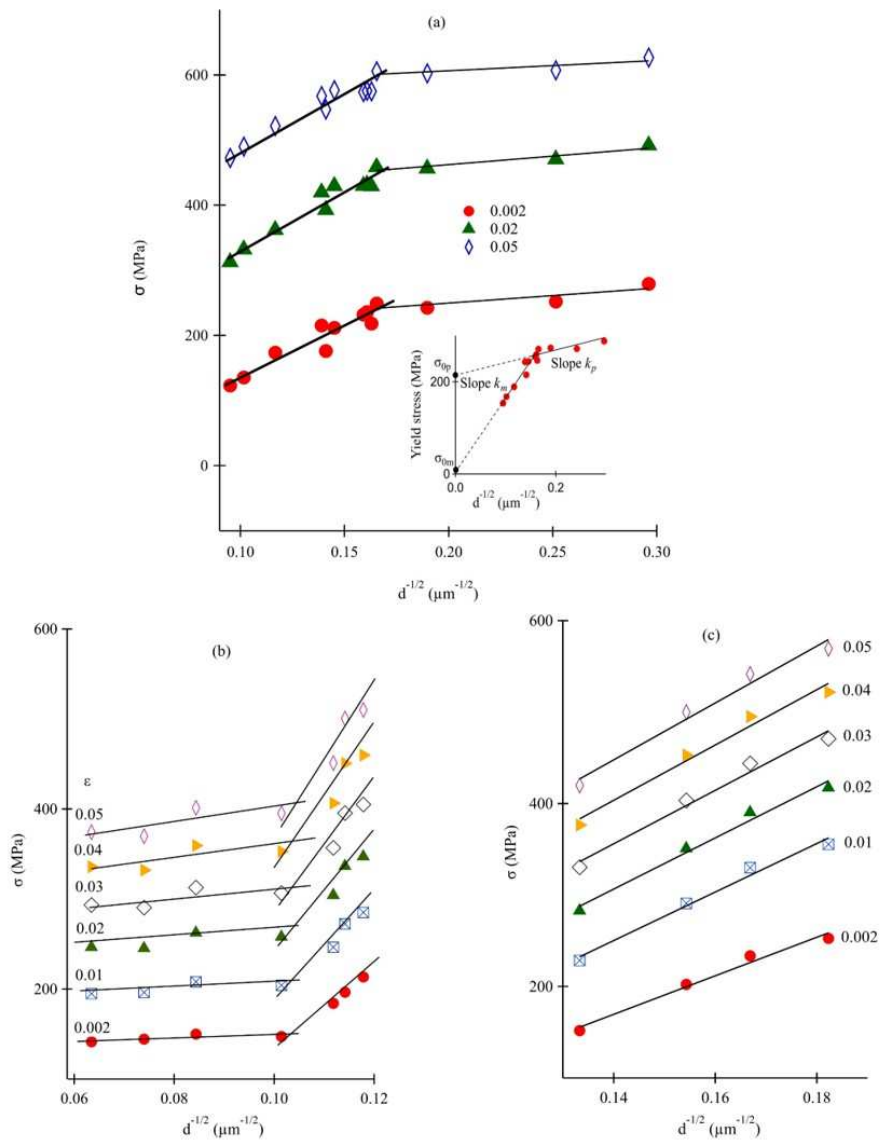


Figure 6 – (a) HP plots for several deformations showing the transition between polycrystalline and multicrystalline behaviors ($t = 500 \mu\text{m}$) (following [51]). In inset, definition of the two distinct stages in HP plot at the yield stress. (b) HP plots for 250 μm in thickness cobalt for different deformation levels showing the transition between multicrystalline and quasi-single crystalline behaviors. (c) HP plots for 125 μm in thickness cobalt exhibiting a multicrystalline single regime in the overall studied ranges of grain size and plastic deformation.

The evolution of the ratio k_m/k_p with the strain presents two distinct stages (Fig. 7(a)). It remains constant until $\varepsilon = 0.025$ and strongly increases for higher values of the strain. This could be related to the modification of the straining mechanisms with the generalization of twinning process, more sensitive to grain size than slip mechanisms [27, 52]. The value of σ_0 in the multicrystalline regime (called σ_{0m}) is of the order of a few MPa at the yield stress, related to the critical resolved shear stress in the basal plane of hcp ideal structures [53]. The ratio σ_{0m}/σ_{0p} is always less than the unity, increases with the deformation (Fig. 7(b)), and tends to saturate at higher strain levels with the generalization of the twinning process. The difference between the mechanical behavior of multicrystals and polycrystals in slip regime is then reduced with strain in accordance to previous observations concerning nickel [54], aluminum [5], or copper [55] and for surface and core regions of copper single crystals [14].

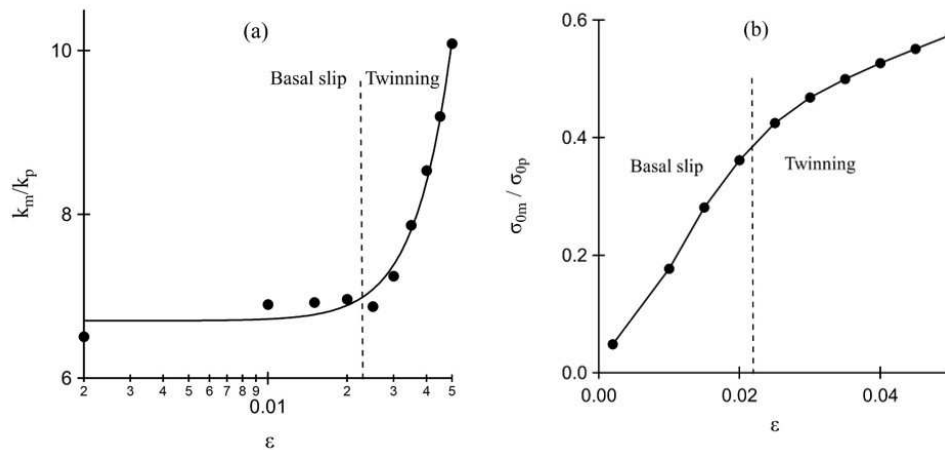


Figure 7 – Evolution of the HP coefficients with deformation for 0.5mm in thickness samples. (a) Ratio k_m/k_p and (b) ratio σ_{0m}/σ_{0p} vs deformation ε .

HP plots for cobalt samples with a thinner thickness of 250 μm are displayed in Fig. 6(b) for several deformations. For this thickness, the t/d ratio ranges between 1 and 3.5 (Table I). Experimental results clearly show two distinct domains which correspond to the transition between multicrystalline and quasi single crystalline regimes. They are separated by a second t/d critical value of around 2.5, which is independent on the strain level. This second critical value was found around unity for nickel [13], and around 2 in Ni-20Cr alloy [56], and seems to slightly increase with a decrease in stacking fault energy. The slope of HP plots is very weak for quasi single crystals. In these samples, grain boundaries are mainly normal to the tensile direction, forming a so-called “bamboo-like” microstructure [57]. It was demonstrated that this grain boundary configuration does not act as strong obstacles to the dislocation slip mechanisms [58]. For 125 μm in thickness samples, t/d ratio is in the range 2.2-4.2. Despite a fewer number of experimental points concerning grain size, HP plots exhibit a single linear behavior independently of the deformation (Fig. 6(c)), with slope values in agreement with the multicrystalline regime.

Fig. 8 displays an overview of the HP law at the yield stress for four thicknesses and a large range of grain size. The multicrystalline regime delimited by the two critical t/d ratio is clearly evidenced despite the scattering of the stress values. In this regime, cobalt experiences a strong softening of its yield stress, of around 40%-50% of the corresponding polycrystalline value. The transitions surprisingly appear for a given grain size, respectively around 30 μm for the first transition and 90 μm for the second one, independently of the thickness, leading therefore to different critical t/d ratio (see inset in Fig.8).

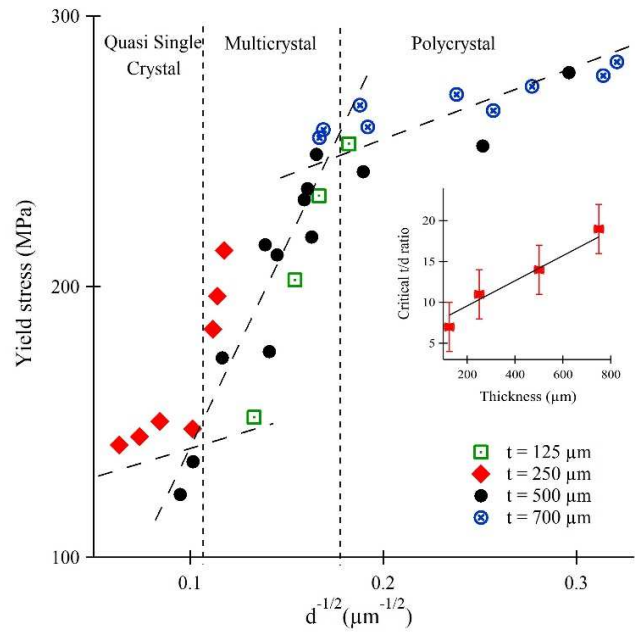


Figure 8 – Initial HP plots for four distinct thicknesses showing the existence of the three crystalline configurations. In inset, evolution of the critical t/d ratio between multicrystalline and polycrystalline stages in function of the thickness.

3.4. Evolution of the strengthening parameters with t/d ratio

The initial work hardening rate θ_0 at the beginning of the plasticity (*i.e.* for a plastic strain of 0.002, see Fig. 5) exhibits three distinct stages with a decrease in t/d ratio (Fig. 9(a)). These stages are delimited by critical t/d ratio taking values in the same order than those depicted in HP plots. However, these critical parameters are independent of the thickness of the samples, highlighting a purely t/d effect on strengthening mechanisms of cobalt. In the polycrystalline regime (t/d higher than a critical value around 10-15), the slope Δ_A of the first stage decreases when the grain size increases (Fig. 9(b)), due to the impact of the grain size on the basal slip mechanism in hcp crystals [59]. Δ_A decreases more

significantly when t/d decreases below the first critical t/d ratio, revealing the size effect on slip process in the multicrystalline regime. By contrast, the slope Δ_B of the second work hardening stage, driven by twinning mechanisms, remains roughly constant with t/d ratio (Fig. 9(b)). Its value is very weak, around 5000 MPa, and the experimental dispersion does not allow highlighting several distinct stages.

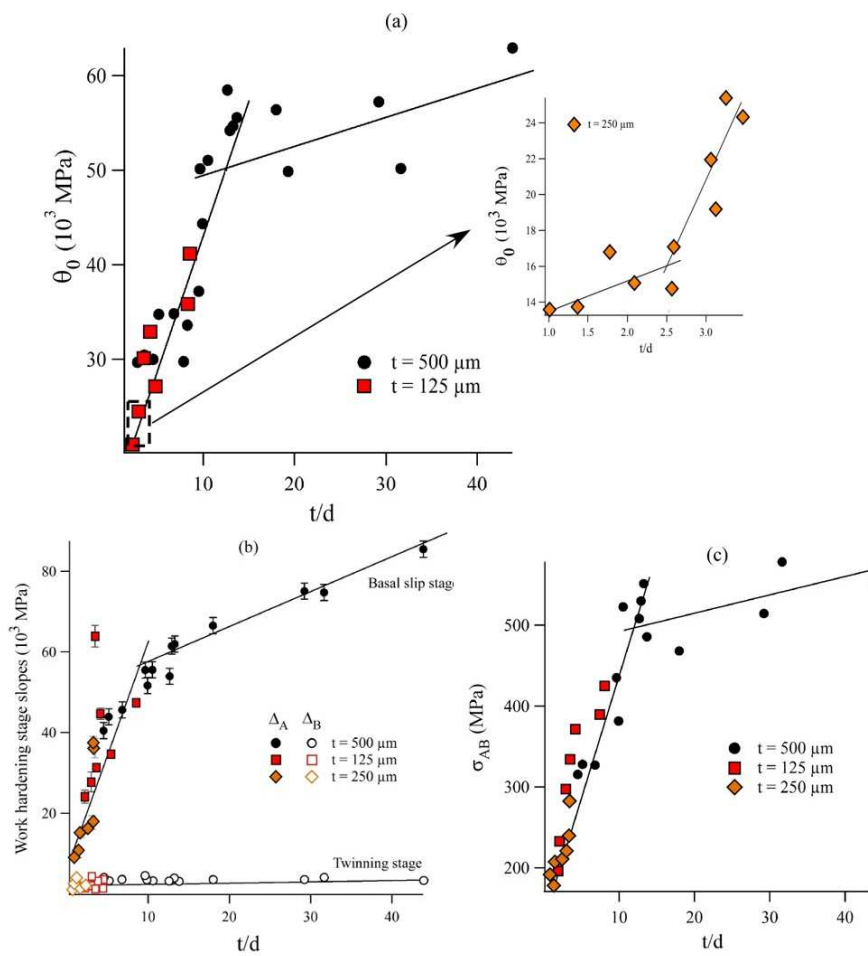


Figure 9 – Evolution of the hardening parameters with t/d ratio computed from Fig. 5. (a) Initial work hardening rate θ_0 , (b) absolute values of slopes Δ in stages A and B, (c) stress transition σ_{AB} between stages A and B.

Size effects in cobalt have a major impact on the yield stress and the basal slip stage, affecting all work hardening parameters until the generalization of twinning mechanisms. This suggests a specific dislocation activity in multicrystals coupled with the apparition of twinning for lower stress values. The evolution of the threshold stress σ_{AB} between the stages A and B supports this observation: this parameter strongly decreases when t/d ratio ranges in the multicrystal regime (Fig. 9(c)), independently on the thickness of samples. The transition for polycrystals to multicrystals in cobalt provokes a progressive extinction of glide mechanisms to the benefit of the twinning process. For quasi-single crystals, twinning is predominant on the overall of plastic strain range.

3.5. Strengthening behavior: slip versus twin mechanisms

The main modes of deformation of cobalt consist of basal slip mechanisms in stage A and generalization of the twinning process in stage B [39]. Numerous parallel slip lines can be observed on the sample surface in the beginning of deformation (Fig. 10(a)), alongside with some deformation twins, already present at this deformation level. Depending on the angle between the c-axis and the normal of the plane samples, one or two activated slip systems are revealed. The basal texture, which develops after rolling and annealing, is detrimental to the simultaneous activation of the three slip systems in the basal plane. Whatever the t/d ratio, glide mechanisms always begin with massive dislocation motion in the basal plane [40]. Multiplication of such mobile dislocations lead to an efficient source of acoustic emission [60, 61]. Planar dislocation configurations are

frequently observed, consisting in pile-ups of single straight dislocation segments against grain or twin boundaries. Two examples of this configuration are depicted in Fig 10(b). These mobile dislocations were identified as $\langle a \rangle$ -type basal perfect dislocations. Sessile $\langle c \rangle$ -type dislocations in dipolar configurations, lying in the prismatic planes, are also sometimes observed [62]. There are less frequently encountered than $\langle a \rangle$ -type ones.

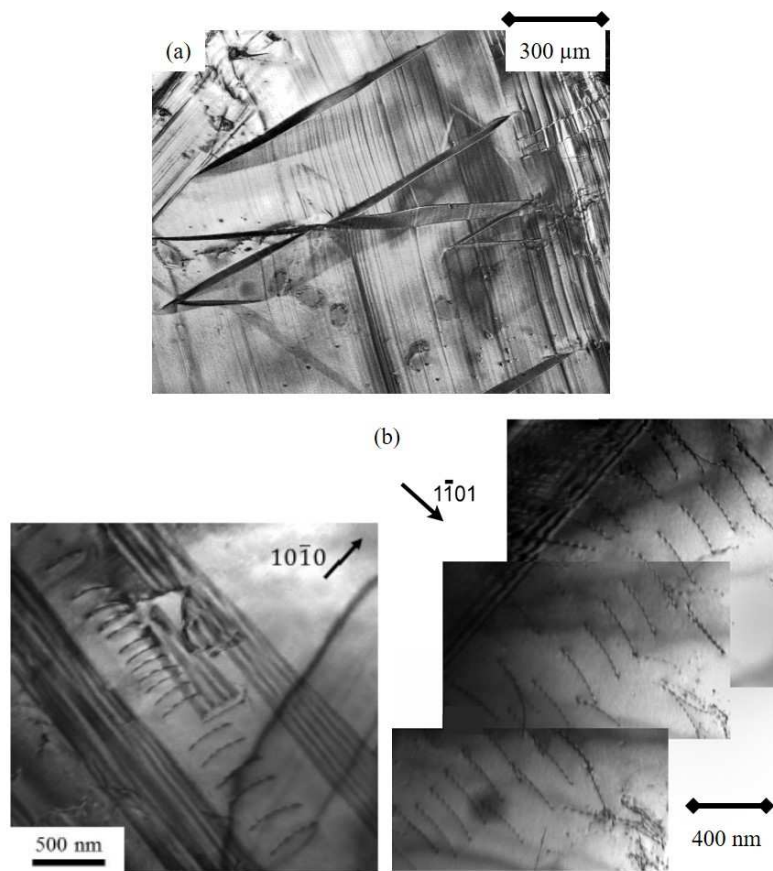


Figure 10 – Microstructural features of gliding mechanisms in cobalt. (a) Slip lines against twins in the beginning of plastic strain, confocal microscopy observation of a multicrystal. (b) Two examples of dislocation pile-ups representative of slip mechanisms in stage A of cobalt polycrystals.

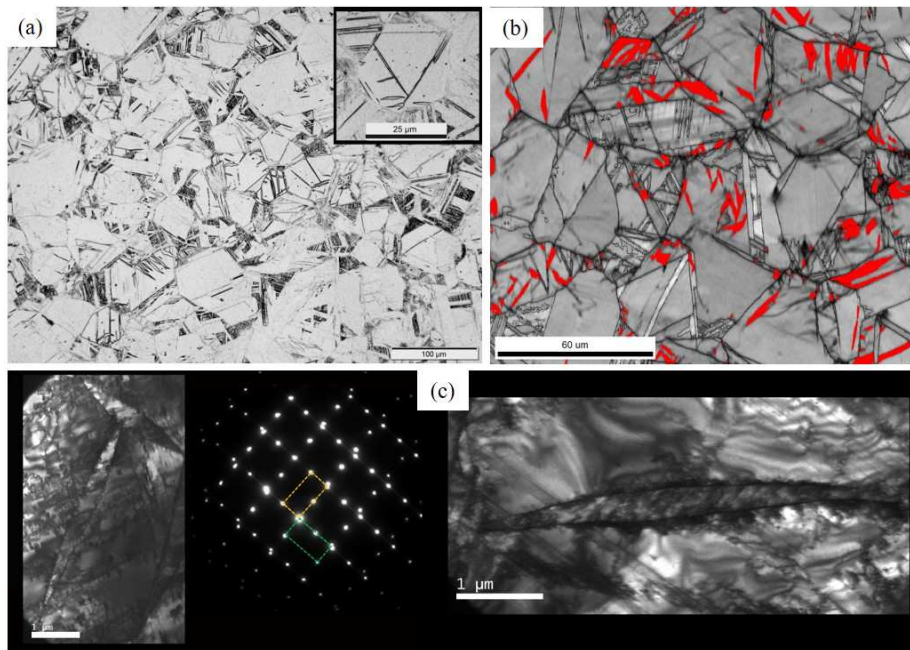


Figure 11 – Microstructural features of twinning mechanisms in polycrystalline cobalt. (a) Twinning generalization in fractured samples observed in optical microscopy. (b) Image Quality map of twins in stage B, the extension twins highlighted in red represent the $\{10\bar{1}2\}$ mode. (c) TEM image of $\{10\bar{1}2\}$ twins, and identification by electron diffraction. The diffraction pattern of the matrix (represented in green) and the twin (represented in yellow) are superposed and show a rotation about the $\langle 1\bar{2}10 \rangle$ axis of $\sim 86^\circ$.

At fracture, generalization of twinning mechanisms is clearly observable (Fig. 11(a)). In between, the progressive apparition of twinning occurs at the end of stage A and during stage B of work hardening. The more frequently activated twin family is the $\{10\bar{1}2\}$ extension mode as evidenced by a precedent statistical work [63]. Fig. 11(b) shows an EBSD map in which the $\{10\bar{1}2\}$ twins are highlighted in red. This twin mode is also formerly identified by TEM observations and analysis of dislocation patterns. Fig. 11(c) shows several twins with lenticular morphology. A typical selected diffraction pattern used for the identification of twins is also depicted in the same figure. The rotation between the

matrix and the twin about the $\langle 1\bar{2}10 \rangle$ axis is 86° , so that this correspond to a $\{10\bar{1}2\}$ twin type.

Decreasing the t/d ratio clearly affect the gliding mechanisms in stage A as evidenced by the evolution of the work hardening parameters (Fig. 9). Such size effects are much less sensitive in stage B because twining mechanisms lead to a refinement of the microstructure and grain size is no longer the pertinent length scale. Pile-ups are the more frequent dislocation arrangement in stage A of polycrystals, due to the low stacking fault energy of cobalt. When the t/d ratio is reduced below the multicrystal critical value, pile-ups remain present as revealed by TEM observations, but are shorter in length and contain more dislocations in average. This feature suggests a significant different work hardening process operating in cobalt when t/d falls below the critical ratio.

In front of pile-ups, an internal stress develops, which can be roughly estimated based on the geometrical properties of the dislocation arrangement (Fig. 12).

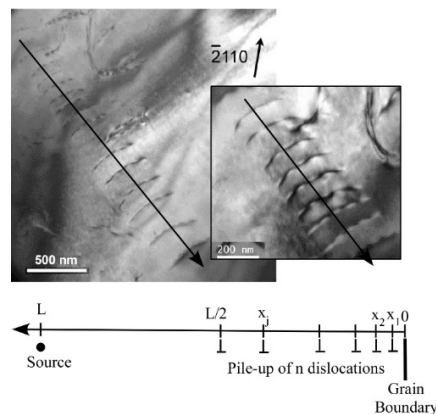


Figure 12 – Example of a pile-up observed by TEM and schematic representation of a pile-up of length L containing n dislocations against a boundary.

Knowing the length L of a pile-up and their number n of dislocations, the internal stress in front of pile-ups can be represented by the local activation shear stress $\Delta\tau$, computed with the relation [64, 65]:

$$\Delta\tau = \frac{nKb}{L} \quad (2)$$

$\Delta\tau = \tau - \tau_i$ with τ the applied shear stress in the slip plane and along the slip direction, and τ_i the minimum internal stress needed to move dislocations along the slip direction. The constant K depends on the screw or edge character of the dislocations. For each pile-up, an image can be obtained using different diffraction vectors and the [0001] zone axis of the corresponding grain. The orientation of the Burgers vector of the dislocations inside pile-ups can be therefore identified. These dislocations are always of mixed character with an angle $\varphi \cong 30^\circ$ between Burgers vector and unit line vector. For such mixed dislocation in an isotropic medium, K takes the following form [66]:

$$K = \frac{\mu[\sin^2 \varphi + (1-\nu) \cos^2 \varphi]}{\pi(1-\nu)} \quad (3)$$

Considering a Poisson's coefficient about 0.31, a Coulomb modulus $\mu = 83.5$ GPa and $\varphi = 30^\circ$, K is equal to 14780 MPa.

Around twenty pile-ups were carefully selected in TEM observations of samples issued from a polycrystal ($t/d = 50$) and a multicrystal ($t/d = 5$) strained in the beginning of the stage A of work-hardening (strain of about 7.10^{-3}). Pile-ups were chosen parallel to the

hole of the thin foil in order to avoid artificial free surface effects. They are also single layers, with all dislocations in the same slip plane, and single-ended, with a source supposed close to a grain boundary and a pile-up against a grain or twin boundary [67]. For each pile up, the total number of dislocations n and their length L were measured. Gliding mechanisms being only activated in the basal plane of cobalt, the value of L was computed taking into account the angle between the observation direction and the [0001] direction. Despite the scattering of measurements, $\Delta\tau$ is found slightly higher in multicrystals (60 ± 20 MPa on average) than in polycrystalline specimens (45 ± 20 MPa on average). For a similar value of strain in stage A, higher mechanical work is then necessary to pile-up dislocations against boundaries in multicrystals.

3.6. Surface effects in multicrystalline samples

Nanoindentation measurements performed across the thickness of multicrystalline samples plastically strained in stage A exhibit a strong decrease in hardness close to the free surfaces (Fig. 13(a)).

The sample corresponding to polycrystalline state and strained in stage A presents an average hardness of 2.8 GPa all across the thickness with no pronounced surface effects (Fig. 13(b)). When it comes to multicrystal sample, in the core region, the same average value of hardness than in polycrystal is observed. However, a significant decrease in hardness on the 100 μm closer to the free surface is highlighted in Fig. 13(b). In this case, taken into account the sample characteristics ($t/d = 5$ and $t = 500 \mu\text{m}$), this feature suggests

that the corresponding stress gradient is only observed in the grain emerging on the free surface.

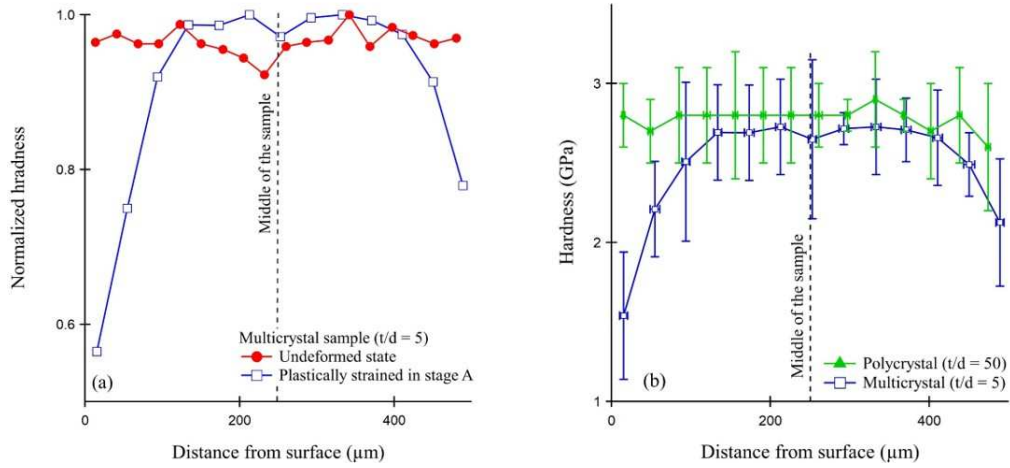


Figure 13 – (a) Normalized hardness values through the thickness of a multocrystal sample not deformed and strained in stage A. (b) Hardness profiles through the thickness of polycrystalline and multocrystalline samples plastically strained in stage A ($t = 500 \mu\text{m}$). Errors bars in Fig. 13(a) are of the same order of magnitude than in Fig. 13(b).

Surface effects can be captured using an analytical composite model, following previous works of Yang *et al* [42]. These authors considered that grains in the surface region behave differently than in the core leading to a mechanical softening of the material close to the free surface. Considering f_s , the volume fraction of the material affected by the surface softening and f_c the volume fraction of core region, not affected by surface effects, the overall stress σ applied to the transverse section can be computed, in first approximation, using the mixture rule between surface and core areas [68]:

$$\sigma = f_s \sigma_s + f_c \sigma_c \quad (4)$$

σ_s and σ_c are the flow stress inside surface and core areas, respectively. For flat plate geometry samples [69], the ratio σ/σ_c can be written under the following form:

$$\frac{\sigma}{\sigma_c} = 1 - \frac{4\alpha d}{w} \left(\frac{1+w/t}{2} - \frac{\alpha d}{t} \right) (1 - \beta) \quad (5)$$

In this equation, α is the number of grains affected by surface effects, β is the ratio between the flow stress of the surface regions over the core ones ($\beta = \sigma_s/\sigma_c$) and w is the width of the specimen, see inset in Fig. 14(a). Eq. (5) was used to fit the evolution of the stress level with deformation and t/d ratio. Results are given in Fig. 14 where each value of stress was normalized by the higher value σ_{max} representative of the polycrystalline stage. It is shown in Fig. 14(a) that surface effects occur for t/d ratio around 15, in agreement with previous results. Moreover, this critical ratio is weakly dependent on the deformation, as observed in HP plots [51].

For each t/d ratio and a given level of deformation, best fits of experimental values are obtained for specific values of α and β . Fig. 14(b) shows that for a polycrystal, α and β are close to 0 and 1, respectively, independent of the deformation, indicating that no surface effects occur. For multicrystals, α is maximal at the yield stress with values around 1.2 for $t/d = 5$ for instance. More than one grain is then affected by size effects when cobalt begins to deform plastically. Surface effects become less pronounced when the deformation increases (α decreases up to 0.5), in agreement with experimental results concerning work

hardening. Correspondingly, β takes its minimum value, showing the strong softening effect of surfaces for multicrystals.

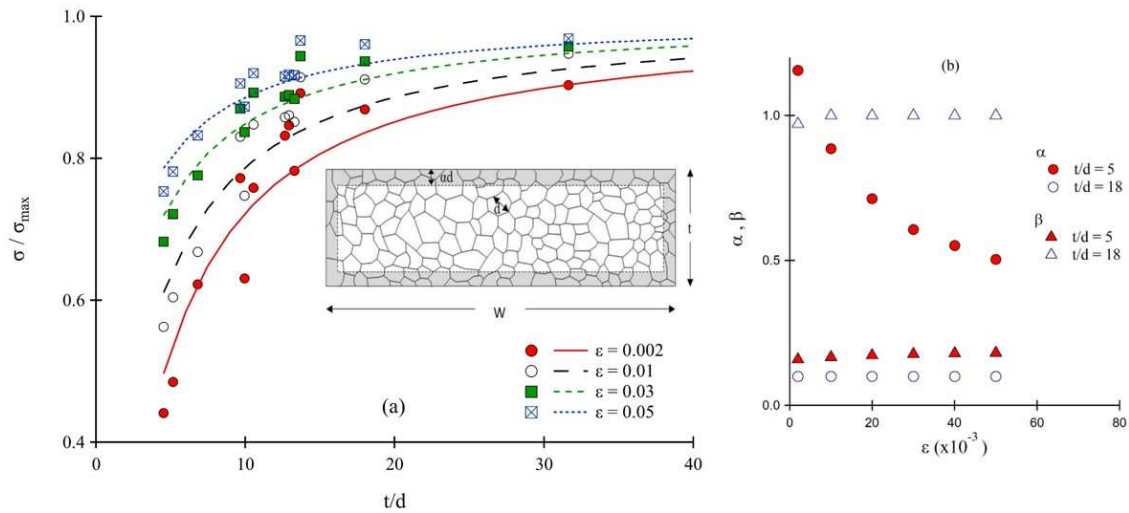


Figure 14 – (a) Evolution of stress with t/d ratio for various plastic strains and corresponding analytical composite model ($t = 500 \mu\text{m}$). In the inset: section of a rectangular flat tensile sample with corresponding geometrical parameters, following Shin and co-workers [69]). (b) Parameters α and β in function of the plastic strain for a multicrystal ($t/d = 5$) and a polycrystal ($t/d = 18$)

4. Discussion

The stronger reduction in stress depicted in HP plots with decreasing grain size when t/d is in the range 2.5-14 (multicrystalline range) is due to a **size effect, which** appears at the end of the elasticity. It was shown in a previous paper [51] that the transition between polycrystals and multicrystals takes place during the microyielding stage of loading. This transition was also recently highlighted by measurements of the magnetic coercive field [18]. Concerning strengthening, all parameters representative **of gliding process are**

affected by the t/d ratio, with a critical value around 12, of the same order than that one found for HP law. Twinning mechanisms are not impacted by such size effects, even if twins are more present in large grain size specimens than in small ones [63].

The size effects in fcc metals were previously closely linked to the stacking fault energy and the ability of cross slip mechanisms during the work hardening [7]. Precedent results concerning nickel [12, 45] and copper [7, 55] also underlined the role of internal stress gradients which develop across the thickness of samples with a decreasing in t/d ratio. This leads to a progressive softening of the surface at the origin of the decrease of stress levels for polycrystals. The softening of the mechanical properties of fcc polycrystals can be attributed to surface effects, the surface becoming progressively softer than the core as the plastic straining proceeds [12]. The physical origin of this softening can be found in the variation of the diameter of cell dislocations between surface and core, higher in the former case than in the latter. The internal stress level being inversely proportional to the cell diameter [70], a gradient of internal stresses progressively takes place through the thickness leading to the overall softening of the mechanical properties.

The low stacking fault energy of cobalt combined with its restricted glide system number imply that this metal is very sensitive to the reduction of the t/d ratio. The composite model of Shin *et al* [69] coupled to nanohardness measurements also highlight an impact of the free surfaces for polycrystalline cobalt. Mechanical softening is mainly detectable during the stage A of work hardening, driven by slip mechanisms in the basal plane.

To better understand the modification of dislocation glide character between polycrystals and polycrystals, work hardening curves of cobalt can be modeled by a one-

parameter model such as that one developed by Mecking [71], Kocks and Mecking [44] or Estrin and Mecking [72]. We have shown in previous works how this model can be successfully used for the study of size effects in fcc materials [43]. In this model, the work hardening is issued from a competition between the progressive storage of dislocations and their annihilation [73]. Following the formulation given by Malygin [74], the general equation of accumulation of dislocations in single crystals, represented by the dislocation density ρ , with the strain γ , takes the following form:

$$\frac{d\rho}{d\gamma} = \kappa_m + \kappa_f \sqrt{\rho} - \kappa_a \rho \quad (6)$$

$\kappa_m = 1/(b\Lambda)$ is the coefficient of multiplication of dislocations in the easy glide stage, when all dislocations slip along one activated gliding system. b is the Burgers vector modulus and Λ the mean free path of mobile dislocations. The second term in the right side of Eq. (6) is an accumulation term related to the athermal storage of mobile dislocations, and the last one is an annihilation component associated with recovery mechanisms such as cross slip. κ_f and κ_a are corresponding constant materials.

The use of this equation can be extended to the case of hexagonal materials if slip mechanisms predominate [25, 75]. The strain hardening of polycrystals can then be studied by the following relationship:

$$(\sigma - \sigma_y)\theta = \frac{1}{2} M^3 \alpha_T^2 \mu^2 b^2 \left[\kappa_m + \kappa_f \left(\frac{\sigma - \sigma_y}{M\alpha\mu b} \right) - \kappa_a \left(\frac{\sigma - \sigma_y}{M\alpha\mu b} \right)^2 \right] \quad (7)$$

σ_y is the yield stress, α_T is a material constant linked to the dislocation arrangement, M is the Taylor factor. The work hardening curves of cobalt can therefore be modeled by a three parameters (A, B and C) adjusted equation [62]:

$$\theta = \frac{A}{\sigma - \sigma_y} + B - C(\sigma - \sigma_y) \quad (8)$$

An example of such a fitting is given in Fig. 15(a). The fitting procedure is robust and stable, weakly dependent on the initial values of A, B and C. B and C are related to κ_f and κ_a , representing multislip gliding and twinning processes, respectively. In the first work hardening stage of cobalt, driven by basal slip mechanisms, the parameter A is especially of interest. It is related to the coefficient of multiplication of dislocation in single slip regime κ_m by the equation:

$$A = \frac{1}{2} M^3 (\alpha_T \mu b)^2 \kappa_m \quad (9)$$

This leads to an expression for the mean free path of mobile dislocations:

$$\Lambda = \frac{M^3 \alpha_T^2 \mu^2 b}{2A} \quad (10)$$

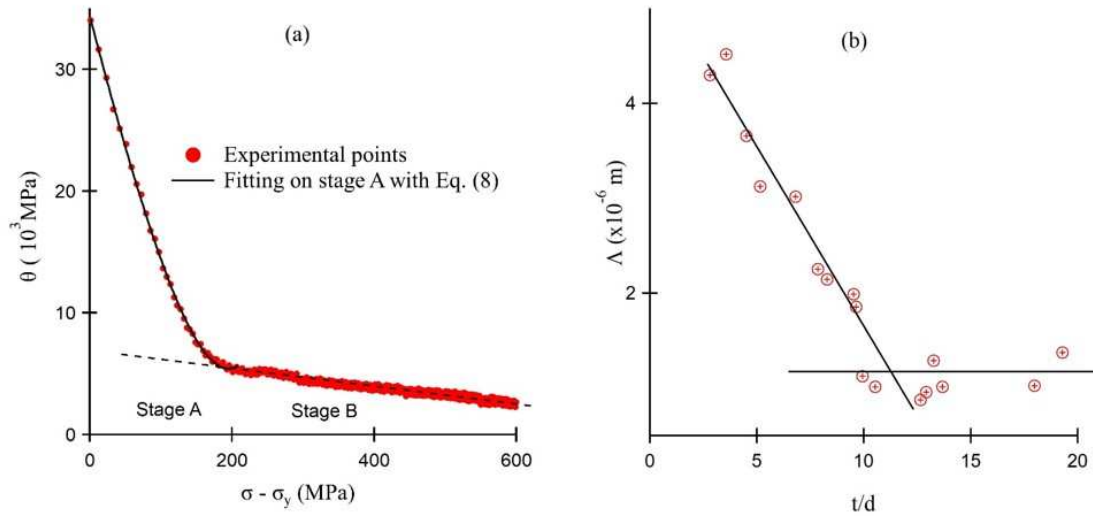


Figure 15 – (a) Modeling of the work hardening curve of cobalt by using Eq. (8) ($t/d = 13$). (b) Evolution of the mean free path of dislocations in stage A with the t/d ratio for cobalt specimens of thickness $500 \mu\text{m}$.

Fig. 15(b) displays the evolution of Λ with t/d for cobalt samples of $500 \mu\text{m}$ in thickness. Λ was computed using $\alpha_T = 0.3$, which holds for pile-ups configurations, $M = 2.3$, considering basal glide of a hcp material moderately textured [76], $\mu = 83.5 \text{ GPa}$ and $b = 0.25 \text{ nm}$. Λ remains constant for polycrystalline specimens, around a mean value of $1.5 \mu\text{m}$. When t/d becomes lower than the critical ratio $(t/d)_c = 14$, a strong increase of Λ is evidenced. This result is similar than that one reported in multicrystalline nickel [11], and numerically predicted by Kocks - Mecking analysis [43]. The slip characteristics in the stage A of work hardening are then deeply modified in the multicrystalline regime. Indeed, increasing the mean free path of dislocations would imply an overall softening of the mechanical properties.

To sum up, the mechanical softening in cobalt multicrystals strongly modifies the yield stress with a pronounced three stages on the HP law (Fig. 8). This softening is also

evidenced by an initial strain hardening rate θ_0 smaller for multicrystals than for polycrystals (Fig. 9(a)) and remains present in the first work hardening stage (Fig. 9(b)). Cobalt multicrystals are then initially softer from a mechanical point of view. When plastic strain occurs, dislocation activity is more important, in good agreement with the increase of the mean free path below the critical t/d ratio (Fig. 15(b)). The internal stress generated around pile-ups by this dislocation activity is then slightly higher in multicrystals, as computed using TEM observations. The overall softening of the mechanical properties of cobalt multicrystals is then due to very strong surface effects, which compensate the small increase of internal stress in the volume. Such effects are the consequence of the greater dislocation mobility, as shown by the increase of the mean free path. Dislocations are able to escape through free surfaces, especially when the grain size is larger. With the generalization of twinning, twins develop also on the free surface of samples. These twins prevent the escape of dislocations. Mechanical behavior of multicrystals and polycrystals tend to become similar when the deformation level is enough for activating the second stage of the work hardening.

5. Conclusion

In this work, the mechanical properties of cobalt were reported for a wide range of grain size and for several sample thicknesses. The transition between polycrystalline and multicrystalline behavior has been demonstrated, occurring for critical number of grains through the thickness of the order of 13-15. The mechanical behavior of cobalt is strongly impacted for t/d ratio less than this critical value, both from the point of view of the

hardening effect of the **grains, related** to a strong modification of the **HP law**, and of dislocation hardening mechanisms in the basal slip stage. It was also demonstrated that the size effects tend to disappear when twinning mechanisms become predominant.

As in fcc metals, the size effects depicted in cobalt **traduce** the existence of an important surface effect inside the samples with less than 13-15 grains through the thickness. The dislocation activity was found to be greater in cobalt multicrystals, leading to denser and smaller dislocation pile-ups, generating larger internal stresses. **Surface effects, therefore, compensate** these larger levels in multicrystals, leading to their overall softening in terms of mechanical properties.

The origin of the strong softening of cobalt at the beginning of plasticity, however, remains unclear. In particular, the role played by nonlinear elasticity during elastic loading and in the microyielding stage needs to be better understood and should be the subject of future research.

Acknowledgments

Part of the experimental work was performed in the PhD work of Gwendoline Fleurier, Normandie Université, UNICAEN, 2016.

References

- [1] E. Arzt, Size effects in materials due to microstructural and dimensional constraints: a comparative review, *Acta Mater.* 46(16) (1998) 5611-5626.
- [2] R.W. Armstrong, On size effects in polycrystal plasticity, *J. Mech.Phys. Sol.* 9 (1961) 196-199.
- [3] R.W. Armstrong, 60 years of Hall-petch: past to present nano-scale connections, *Mater. Trans.* 55(1) (2014) 2-12.
- [4] T. Fulop, W.A.M. Brekelmans, M.G.D. Geers, Size effects from grain statistics in ultra-thin metal sheets, *J. Mat. Proc. Techn.* 174(1-3) (2006) 233-238.

- [5] P.J.M. Janssen, T.H. de Keijser, M.G.D. Geers, An experimental assessment of grain size effects in the uniaxial straining of thin Al sheet with a few grains across the thickness, *Mater. Sci. Eng. A* 419(1-2) (2006) 238-248.
- [6] S. Miyazaki, K. Shibata, H. Fujita, Effect of specimen thickness on mechanical properties of polycrystalline aggregates with various grain sizes, *Acta Metall.* 27 (1979) 855-862.
- [7] E. Hug, P.A. Dubos, C. Keller, L. Duchêne, A.M. Habraken, Size effects and temperature dependence on strain-hardening mechanisms in some face centered cubic materials, *Mech. Mater.* 91, Part 1 (2015) 136-151.
- [8] A.W. Thompson, M.I. Baskes, W.F. Flanagan, The dependence of polycrystal work hardening on grain size, *Acta Metall.* 21 (1973) 1017-10128.
- [9] P.A. Dubos, E. Hug, S. Thibault, M.B. Bettaieb, C. Keller, Size effects in thin face centered cubic metals for different complex forming loadings, *Metall. Mater. Trans. A* 44(12) (2013) 5478-5487.
- [10] C. Keller, E. Hug, A.M. Habraken, L. Duchêne, Effect of stress path on the miniaturization size effect for nickel polycrystals, *Int. J. Plast.* 64(0) (2015) 26-39.
- [11] E. Hug, C. Keller, Intrinsic Effects due to the Reduction of Thickness on the Mechanical Behavior of Nickel Polycrystals, *Metall. Mater. Trans. A* 41(10) (2010) 2498-2506.
- [12] C. Keller, E. Hug, A.M. Habraken, L. Duchene, Finite element analysis of the free surface effects on the mechanical behavior of thin nickel polycrystals, *Int. J. Plast.* 29 (2012) 155-172.
- [13] C. Keller, E. Hug, X. Feaugas, Microstructural size effects on mechanical properties of high purity nickel, *Int. J. Plast.* 27 (2011) 635-654.
- [14] J.T. Fourie, The flow stress gradient between the surface and centre of deformed copper single crystals, *Philos. Mag.* 17 (1967) 735-756.
- [15] C. Keller, A.M. Habraken, L. Duchene, Finite element investigation of size effects on the mechanical behavior of nickel single crystals, *Mater. Sci. Eng. A* 550(0) (2012) 342-349.
- [16] X.L. Geng, B. Wang, Y.J. Zhang, J.X. Huang, M.M. Duan, K.S. Zhang, Effect of crystalline anisotropy and forming conditions on thinning and rupturing in deep drawing of copper single crystal, *J. Mat. Proc. Techn.* 213(4) (2013) 574-580.
- [17] L.V. Raulea, A.M. Goijaerts, L.E. Govaert, F.P.T. Baaijens, Size effects in the processing of thin metal sheets, *J. Mat. Proc. Techn.* 115(1) (2001) 44-48.
- [18] E. Hug, C. Keller, Size effects and magnetoelastic couplings: a link between Hall–Petch behaviour and coercive field in soft ferromagnetic metals, *Philos. Mag.* (2019) 1-30.
- [19] K. Mohri, T. Uchiyama, L.P. Shen, C.M. Cai, L.V. Panina, Sensitive micro magnetic sensor family using magneto-impedance (MI) and stress-impedance (SI) effects for intelligent measurements and controls, *Sens. Actuators A* 91 (2001) 85-90.
- [20] S. Chauhan, A.F. Bastawros, Probing thickness-dependent dislocation storage in freestanding Cu films using residual electrical resistivity, *Appl. Phys. Letters* 93 (2008) 041901.
- [21] J.W. Lim, M. Isshiki, Electrical resistivity of Cu films deposited by ion beam deposition: Effects of grain size, impurities, and morphological defect, *J. Appl. Phys.* 99(9) (2006) 094909.
- [22] H. Dong, B. Wen, R. Melnik, Relative importance of grain boundaries and size effects in thermal conductivity of nanocrystalline materials, *Scient. Rep.* 4 (2014) 7037.
- [23] C.M. Byer, K.T. Ramesh, Effects of the initial dislocation density on size effects in single-crystal magnesium, *Acta Mater.* 61(10) (2013) 3808-3818.
- [24] Q. Yu, Z.W. Shan, J. Li, X. Huang, L. Xiao, J. Sun, E. Ma, Strong crystal size effect on deformation twinning, *Nature* 463 (2010) 335-338.
- [25] Y. Qiao, X. Wang, Z. Liu, E. Wang, Effects of grain size, texture and twinning on mechanical properties and work-hardening behaviors of pure Mg, *Mater. Sci. Eng. A* 578 (2013) 240-246.
- [26] S.V. Ramani, P. Rodriguez, Grain size dependence of the deformation behaviour of alpha zirconium, *Canad. Metal. Quarterly* 11(1) (1972) 61-67.
- [27] A. Ghaderi, M.R. Barnett, Sensitivity of deformation twinning to grain size in titanium and magnesium, *Acta Mater.* 59(20) (2011) 7824-7839.
- [28] N. Ono, R. Nowak, S. Miura, Effect of deformation temperature on Hall–Petch relationship registered for polycrystalline magnesium, *Mater. Letters* 58(1) (2004) 39-43.
- [29] M.A. Meyers, O. Vohringer, V.A. Lubarda, The onset of twinning in metals: a constitutive description, *Acta Mater.* 49(19) (2001) 4025-4039.

- [30] Z. Fan, The grain size dependence of ductile fracture toughness of polycrystalline metals and alloys, *Mater. Sci. Eng. A* 191(1) (1995) 73-83.
- [31] M.R. Barnett, Z. Keshavarz, A.G. Beer, D. Atwell, Influence of grain size on the compressive deformation of wrought Mg-3Al-1Zn, *Acta Mater.* 52 (2004) 5093-5103.
- [32] X.Y. Lou, M. Li, R.K. Boger, S.R. Agnew, R.H. Wagoner, Hardening evolution of AZ31B Mg sheet, *Int. J. Plast.* 23(1) (2007) 44-86.
- [33] H. Nasiri-Abarbekoh, A. Ekrami, A.A. Ziaei-Moayyed, Effects of thickness and texture on mechanical properties anisotropy of commercially pure titanium thin sheets, *Mater. Design* 44 (2013) 528-534.
- [34] N.R. Ecob, B. Ralph, Effect of grain size on flow stress of textured Zn alloy, *Metal Science* 17(7) (1983) 317-324.
- [35] W. Betteridge, The properties of metallic cobalt, *Prog. Mater. Sci.* 24 (1979) 51-142.
- [36] A. Couret, D. Caillard, An in situ study of prismatic glide in magnesium—I. The rate controlling mechanism, *Acta Metall.* 33(8) (1985) 1447-1454.
- [37] K. Máthi, K. Nyilas, A. Axt, I. Dragomir-Cernatescu, T. Ungár, P. Lukáč, The evolution of non-basal dislocations as a function of deformation temperature in pure magnesium determined by X-ray diffraction, *Acta Mater.* 52(10) (2004) 2889-2894.
- [38] V.M. Marx, C. Kirchlechner, B. Breitbach, M.J. Cordill, D.M. Töbrens, T. Waitz, G. Dehm, Strain-induced phase transformation of a thin Co film on flexible substrates, *Acta Mater.* 121 (2016) 227-233.
- [39] A. Seeger, S. Mader, H. Kronmüller, Theory of work-hardening of FCC and HCP single crystals, in: J.W. G. Thomas (Ed.), *Electron microscopy and strength of crystals*, Interscience Publishers, New-York, 1963, pp. 665-712.
- [40] M. Martinez, G. Fleurier, F. Chmelík, M. Knapek, B. Viguier, E. Hug, TEM analysis of the deformation microstructure of polycrystalline cobalt plastically strained in tension, *Mater. Charact.* 134(Supplement C) (2017) 76-83.
- [41] P.G. Partridge, The crystallography and deformation modes of hexagonal close-packed metals, *Metall. Rev.* 12 (1967) 169-194.
- [42] B. Yang, C. Motz, M. Rester, G. Dehm, Yield stress influenced by the ratio of wire diameter to grain size – a competition between the effects of specimen microstructure and dimension in micro-sized polycrystalline copper wires, *Philos. Mag.* 92(25-27) (2012) 3243-3256.
- [43] C. Keller, E. Hug, Kocks-Mecking analysis of the size effects on the mechanical behavior of nickel polycrystals, *Int. J. Plast.* 98 (2017) 106-122.
- [44] U.F. Kocks, H. Mecking, Physics and phenomenology of strain hardening: the FCC case, *Prog. Mater. Sci.* 48(3) (2003) 171-273.
- [45] C. Keller, E. Hug, D. Chateigner, On the origin of the stress decrease for nickel polycrystals with few grains across the thickness, *Mater. Sci. Eng. A* 500(1-2) (2009) 207-215.
- [46] G. Bouquet, B. Dubois, Influence of the f.c.c. phase retained at room temperature on the mechanical properties of cobalt, *Scripta Metall.* 12 (1978) 1079-1081.
- [47] A. Korner, H.P. Karnthaler, Weak-beam study of glide dislocations in h.c.p. cobalt, *Phil. Mag. A* 48(3) (1983) 469-477.
- [48] N. Stanford, U. Carlson, M.R. Barnett, Deformation twinning and the Hall-Petch relation in commercial purity Ti, *Metall. Mater. Trans. A* 39 (2008) 934-944.
- [49] A.W. Thompson, Use of non-polycrystal specimens in mechanical behaviour tests, *Scripta Metall.* 8 (1973) 145-148.
- [50] C.C. Sanderson, *Deformation of polycrystalline cobalt*, Department of Metallurgy, The University of British Columbia, Vancouver, 1972, p. 198.
- [51] G. Fleurier, E. Hug, M. Martinez, P.-A. Dubos, C. Keller, Size effects and Hall-Petch relation in polycrystalline cobalt, *Phil. Mag. Letters* 95 (2015) 122-130.
- [52] M. Arul Kumar, M. Wroński, R.J. McCabe, L. Capolungo, K. Wierzbowski, C.N. Tomé, Role of microstructure on twin nucleation and growth in HCP titanium: A statistical study, *Acta Mater.* 148 (2018) 123-132.
- [53] B. Hutchinson, J. Jain, M.R. Barnett, A minimum parameter approach to crystal plasticity modelling, *Acta Mater.* 60(15) (2012) 5391-5398.
- [54] C. Keller, E. Hug, Hall-Petch behaviour of Ni polycrystals with a few grains per thickness, *Mater. Letters* 62(10-11) (2008) 1718-1720.

- [55] E. Hug, P.A. Dubos, C. Keller, Temperature dependence and size effects on strain hardening mechanisms in copper polycrystals, *Mater. Sci. Eng. A* 574(0) (2013) 253-261.
- [56] M. Rudloff, Etude des mécanismes de transition volume / surface du comportement mécanique d'un alliage Ni20Cr, PhD Thesis, Université de Technologie de Compiègne, 2010, p. 199.
- [57] P.J.M. Janssen, J.P.M. Hoefnagels, T.H. de Keijser, M.G.D. Geers, Processing induced size effects in plastic yielding upon miniaturisation, *J. Mech.Phys. Sol.* 56(8) (2008) 2687-2706.
- [58] Y. Sutou, T. Omori, K. Yamauchi, N. Ono, R. Kainuma, K. Ishida, Effect of grain size and texture on pseudoelasticity in Cu–Al–Mn-based shape memory wire, *Acta Mater.* 53(15) (2005) 4121-4133.
- [59] T.B. Britton, F.P.E. Dunne, A.J. Wilkinson, On the mechanistic basis of deformation at the microscale in hexagonal close-packed metals, *Proc. Roy. Soc. A* 471(2178) (2015).
- [60] C.R. Heiple, S.H. Carpenter, Acoustic emission produced by deformation of metals and alloys - A review : Part I, *J. Acoust. Emission* 6(3) (1987) 177-204.
- [61] C.R. Heiple, S.H. Carpenter, Acoustic emission produced by deformation of metals and alloys - A review : Part II, *J. Acoust. Emission* 6(4) (1987) 215-237.
- [62] G. Fleurier, Etude des transitions volume / surface des propriétés mécaniques du cobalt de haute pureté. Influence des mécanismes de glissement et de maillage, PhD, Normandie Université, UNICAEN, 2016.
- [63] M. Martinez, E. Hug, Characterization of deformation twinning in polycrystalline cobalt: A quantitative analysis, *Materialia* 7 (2019) 100420.
- [64] W. Cai, W.D. Nix, Imperfections in crystalline solids, Cambridge University Press 2016.
- [65] J. Friedel, Dislocations, Pergamon Press 1964.
- [66] J.P. Hirth, J. Lothe, Theory of dislocations, second ed., Krieger publishing company, Malabar, Florida, 1992.
- [67] J.C.M. Li, Y.T. Chou, The role of dislocations in the flow stress grain size relationships, *Metal. Mater. Trans. B* 1(5) (1970) 1145.
- [68] J.T. Fourie, Soft surface effect in copper single crystals oriented for multiple glide and in polycrystalline copper, Strength of metals and alloys 7th international conference, Pergamon Press, 1986, pp. 99-104.
- [69] C. Shin, S. Lim, H.-h. Jin, P. Hosemann, J. Kwon, Specimen size effects on the weakening of a bulk metastable austenitic alloy, *Mater. Sci. Eng. A* 622(0) (2015) 67-75.
- [70] D. Kuhlmann-Wilsdorf, Theory of plastic deformation: properties of low energy dislocation structures, *Mater. Sci. Eng. A* 113 (1989) 1-41.
- [71] H. Mecking, Description of hardening curves of fcc single and polycrystals, in: A.W. Thompson (Ed.), Work hardening in tension and fatigue, TMS-AIME, New-York, 1977, pp. 67-88.
- [72] Y. Estrin, H. Mecking, A unified phenomenological description of work hardening and creep based on one-parameter models, *Acta Metall.* 32(1) (1984) 57-70.
- [73] J. Gil Sevillano, Flow stress and work hardening, in: H. Mughrabi (Ed.), Plastic deformation and fracture of materials, VCH Verlagsgesellschaft mbH, VCH Publishers Inc., Weinheim, New York, 1993, pp. 19-88.
- [74] G.A. Malygin, Dislocation Density Evolution Equation and Strain Hardening of f.c.c. Crystals, *Phys. Stat. Sol. A* 119(2) (1990) 423-436.
- [75] R. Král, Z. Trojanová, P. Lukáč, Softening during Deformation of Zr Alloys, *Key Eng. Mater.* 97-98 (1995) 359-364.
- [76] C.H. Cáceres, P. Lukáč, Strain hardening behaviour and the Taylor factor of pure magnesium, *Philos. Mag.* 88(7) (2008) 977-989.